Continuous-wave watt-level Nd:YLF/KGW Raman laser operating at near-IR, yellow and lime-green wavelengths

Jonas Jakutis-Neto,[1,2,*] Jipeng Lin,[1] Niklaus Ursus Wetter,[2] and Helen Pask[1]

[1]*MQ Photonics Research Centre, Department of Physics, Macquarie University, Sydney, NSW 2109, Australia*
[2]*Instituto de Pesquisas Energéticas e Nucleares, CNEN/SP, Universidade de São Paulo, CEP 05508-000, São Paulo/SP, Brazil*
**jonas.jakutis-neto@mq.edu.au*

Abstract: A Nd:YLF/KGW Raman laser has been investigated in this work. We have demonstrated CW output powers at six different wavelengths, 1147 nm (0.70 W), 1163 nm (0.95 W), 549 nm (0.65 W), 552 nm (1.90 W), 573 nm (0.60 W) and 581 nm (1.10 W), with higher peak powers achieved under quasi-CW operation. Raman conversion of the 1053 nm fundamental emission is reported for the first time, enabling two new wavelengths in crystalline Raman lasers, 549 nm and 552 nm. The weak thermal lensing associated with Nd:YLF has enabled to achieve good beam quality, $M^2 \leq 2.0$, and stable operation in relatively long cavities.

OCIS codes: (140.3550) Lasers, Raman; (140.3580) Lasers, solid-state; (140.7300) Visible lasers; (140.3530) Lasers, neodymium.

References and links

1. A. S. Grabtchikov, V. A. Lisinetskii, V. A. Orlovich, M. Schmitt, R. Maksimenka, and W. Kiefer, "Multimode pumped continuous-wave solid-state Raman laser," Opt. Lett. **29**(21), 2524–2526 (2004).
2. A. A. Demidovich, A. S. Grabtchikov, V. A. Lisinetskii, V. N. Burakevich, V. A. Orlovich, and W. Kiefer, "Continuous-wave Raman generation in a diode-pumped Nd^{3+}:$KGd(WO_4)_2$ laser," Opt. Lett. **30**(13), 1701–1703 (2005).
3. H. M. Pask, "Continuous-wave, all-solid-state, intracavity Raman laser," Opt. Lett. **30**(18), 2454–2456 (2005).
4. A. J. Lee, H. M. Pask, D. J. Spence, and J. A. Piper, "Efficient 5.3 W cw laser at 559 nm by intracavity frequency summation of fundamental and first-Stokes wavelengths in a self-Raman Nd:$GdVO_4$ laser," Opt. Lett. **35**(5), 682–684 (2010).
5. L. Fan, Y.-X. Fan, Y.-Q. Li, H. Zhang, Q. Wang, J. Wang, and H.-T. Wang, "High-efficiency continuous-wave Raman conversion with a $BaWO_{(4)}$ Raman crystal," Opt. Lett. **34**(11), 1687–1689 (2009).
6. V. G. Savitski, I. Friel, J. E. Hastie, M. D. Dawson, D. Burns, and A. J. Kemp, "Characterization of single-crystal synthetic diamond for multi-watt continuous-wave Raman lasers," IEEE J. Quantum Electron. **48**(3), 328–337 (2012).
7. Y. Lü, W. Cheng, Z. Xiong, J. Lu, L. Xu, G. Sun, and Z. Zhao, "Efficient CW laser at 559 nm by intracavity sum-frequency mixing in a self-Raman Nd:YVO_4 laser under direct 880 nm diode laser pumping," Laser Phys. Lett. **7**(11), 787–789 (2010).
8. A. J. Lee, D. J. Spence, J. A. Piper, and H. M. Pask, "A wavelength-versatile, continuous-wave, self-Raman solid-state laser operating in the visible," Opt. Express **18**(19), 20013–20018 (2010).
9. H. Y. Zhu, Y. M. Duan, G. Zhang, C. H. Huang, Y. Wei, H. Y. Shen, Y. Q. Zheng, L. X. Huang, and Z. Q. Chen, "Efficient second harmonic generation of double-end diffusion-bonded Nd:YVO_4 self-Raman laser producing 7.9 W yellow light," Opt. Express **17**(24), 21544–21550 (2009).
10. V. A. Lisinetskii, A. S. Grabtchikov, A. A. Demidovich, V. N. Burakevich, V. A. Orlovich, and A. N. Titov, "Nd:KGW/KGW crystal: efficient medium for continuous-wave intracavity Raman generation," Appl. Phys. B: Lasers Opt. **88**(4), 499–501 (2007).
11. P. Dekker, H. M. Pask, D. J. Spence, and J. A. Piper, "Continuous-wave, intracavity doubled, self-Raman laser operation in Nd:$GdVO_{(4)}$ at 586.5 nm," Opt. Express **15**(11), 7038–7046 (2007).
12. A. J. Lee, H. M. Pask, P. Dekker, and J. A. Piper, "High efficiency, multi-Watt CW yellow emission from an intracavity-doubled self-Raman laser using Nd:$GdVO_{4,}$," Opt. Express **16**(26), 21958–21963 (2008).
13. Y. M. Duan, H. Y. Zhu, G. Zhang, C. H. Huang, Y. Wei, C. Y. Tu, Z. J. Zhu, F. G. Yang, and Z. Y. You, "Efficient 559.6 nm light produced by sum-frequency generation of diode-end-pumped Nd:YAG/$SrWO_4$ Raman laser," Laser Phys. Lett. **7**(7), 491–494 (2010).
14. M. Pollnau, P. J. Hardman, M. A. Kern, W. A. Clarkson, and D. C. Hanna, "Upconversion-induced heat generation and thermal lensing in Nd:YLF and Nd:YAG," Phys. Rev. B **58**(24), 16076–16092 (1998).

#161668 - $15.00 USD Received 18 Jan 2012; revised 3 Apr 2012; accepted 4 Apr 2012; published 16 Apr 2012

15. Y. F. Lü, X. H. Zhang, A. F. Zhang, X. D. Yin, and J. Xia, "Efficient 1047 nm CW laser emission of Nd:YLF under direct pumping into the emitting level," Opt. Commun. **283**(9), 1877–1879 (2010).
16. W. A. Clarkson, P. J. Hardman, and D. C. Hanna, "High-power diode-bar end-pumped Nd:YLF laser at 1.053 microm," Opt. Lett. **23**(17), 1363–1365 (1998).
17. C. Bollig, C. Jacobs, M. J. D. Esser, E. H. Bernhardi, and H. M. von Bergmann, "Power and energy scaling of a diode-end-pumped Nd:YLF laser through gain optimization," Opt. Express **18**(13), 13993–14003 (2010).
18. Y. K. Bu, C. Q. Tan, and N. Chen, "Continuous-wave yellow light source at 579 nm based on intracavity frequency-doubled Nd:YLF/$SrWO_4$/LBO Raman laser," Laser Phys. Lett. **8**(6), 439–442 (2011).
19. A. A. Kaminskii, K. Ueda, H. J. Eichler, Y. Kuwano, H. Kouta, S. N. Bagaev, T. H. Chyba, J. C. Barnes, G. M. A. Gad, T. Murai, and J. Lu, "M. A. Gad, T. Murai, and J. Lu, "Tetragonal vanadates YVO_4 and $GdVO_4$ - new efficient χ^3-materials for Raman lasers," Opt. Commun. **194**(1-3), 201–206 (2001).
20. P. J. Hardman, W. A. Clarkson, G. J. Friel, M. Pollnau, and D. C. Hanna, "Energy-transfer upconversion and thermal lensing in high-power end-pumped Nd: YLF laser crystals," IEEE J. Quantum Electron. **35**(4), 647–655 (1999).
21. D. C. Hanna, C. G. Sawyers, and M. A. Yuratich, "Telescopic resonators for large-volume TEM_{00}-mode operation," Opt. Quantum Electron. **13**(6), 493–507 (1981).
22. I. V. Mochalov, "Laser and nonlinear properties of the potassium gadolinium tungstate laser crystal $KGd(WO_4)_2:Nd^{3+}$-(KGW:Nd)," Opt. Eng. **36**(6), 1660–1669 (1997).
23. M. E. Innocenzi, H. T. Yura, C. L. Fincher, and R. A. Fields, "Thermal modeling of continuous-wave end-pumped solid-state lasers," Appl. Phys. Lett. **56**(19), 1831–1833 (1990).
24. A. A. Kaminskii, C. L. McCray, H. R. Lee, S. W. Lee, D. A. Temple, T. H. Chyba, W. D. Marsh, J. C. Barnes, A. N. Annanenkov, V. D. Legun, H. J. Eichler, G. M. A. Gad, and K. Ueda, "High efficiency nanosecond Raman lasers based on tetragonal $PbWO_4$ crystals," Opt. Commun. **183**(1-4), 277–287 (2000).
25. G. E. James, E. M. Harrell II, C. Bracikowski, K. Wiesenfeld, and R. Roy, "Elimination of chaos in an intracavity-doubled Nd:YAG laser," Opt. Lett. **15**(20), 1141–1143 (1990).
26. V. Magni, G. Cerullo, S. De Silvestri, O. Svelto, L. J. Qian, and M. Danailov, "Intracavity frequency doubling of a cw high-power TEM_{00} Nd:YLF laser," Opt. Lett. **18**(24), 2111–2113 (1993).

1. Introduction

The ability to generate continuous wave (CW) laser output in the near-infrared region between 1.1 μm and 1.2 μm, and in the yellow-orange range, has seen CW Raman lasers undergo rapid development in the past 7 years. In 2004 the first CW external-resonator crystalline Raman laser was reported by Grabitchikov *et al.* [1], then in 2005, CW intracavity crystalline Raman lasers were reported by, Demidovich *et al.* [2] and Pask [3]. Following these important milestones, multi-Watt CW Raman laser operation in the infrared has been demonstrated using a variety of different Raman crystals such as Nd:$GdVO_4$ [4], $BaWO_4$ [5] and diamond [6]. CW intracavity Raman lasers are built using the same components as conventional diode-pumped solid state lasers (DPSSL), and they have the capacity to generate hard to reach wavelengths. By incorporating intracavity frequency mixing, new wavelengths in the visible can be generated [7]. Further, by generating higher order Stokes intracavity fields via cascading the Stimulated Raman Scattering (SRS) process, wavelength selectable lasers have been demonstrated [8]. The diode to visible efficiency with which these lasers operate is high, typically 10-20% [8], and as such, many groups are pursuing different approaches to improve the performance of CW Raman lasers.

As with conventional DPSSLs, thermal lensing is an important issue in Raman lasers that frequently limits the output powers to which they can be scaled. For Raman lasers there is an additional thermal load due to the inelastic nature of the Raman shifting process, which generates phonons during the wavelength conversion. With the exception of [5], the most efficient CW Raman lasers reported to date tend to be self-Raman lasers, in which the laser crystal itself is Raman active; examples include Nd:$GdVO_4$, Nd:KGW and Nd:YVO_4 lasers [4, 9, 10]. In comparing these self-Raman lasers to Raman lasers with a separate Raman crystal, we can see that the resonator losses are lower, because there are fewer crystal interfaces, and they are as compact as the equivalent fundamental wavelength laser. Yet thermal loading is highest for self-Raman lasers, and the suitable materials (vanadates and tungstates) are not the crystals with best thermal properties. In many cases, it is thermal lensing that limits the maximum output powers that can be achieved from self-Raman lasers [11, 12], and further, such strong thermal lensing can impact on beam quality and restrict cavity design. Distributing the thermal load by using separate laser and Raman crystals, is one approach to manage thermal lensing. In fact the most efficient, multi-Watt, first Stokes laser,

#161668 - $15.00 USD Received 18 Jan 2012; revised 3 Apr 2012; accepted 4 Apr 2012; published 16 Apr 2012

generating 3.36 W at 1180 nm with a diode to first Stokes efficiency of 13.2% was obtained from a Nd:YVO_4/$BaWO_4$ Raman laser [5]. Nd:YAG offers better thermal properties compared to Nd:YVO_4 and Nd:$GdVO_4$, and has been used with some success [13], however Nd:YAG has no naturally-polarized emission, and birefringence loss is detrimental to Raman laser performance. In this work, we have chosen to explore another well-known crystal, Nd:YLF.

The benefits of using Nd:$LiYF_4$ (Nd:YLF) as the fundamental laser crystal in a CW intracavity Raman laser are that it provides a naturally polarized emission and a weak thermal lens [14]. The weak thermal lens is not due to superior thermal conductivity e.g. as in YAG, but rather it arises because the crystal has a negative dn/dT value which partially compensates the positive lens generated from end face bulging. It has π and σ polarized emissions at different wavelengths, 1047 nm and 1053 nm, respectively, shorter than the traditional 1064 nm, thus providing an unusual range of Stokes wavelengths and corresponding visible wavelengths. As a disadvantage it has a low thermal fracture limit, which restricts the maximum absorbed pump power. This can be partly alleviated by using direct excitation of the upper laser level, by means of a diode emitting at 881 nm instead of the usual 806 nm and 797 nm wavelengths typically used to pump Nd:YLF. Pumping directly into the upper laser level eliminates multiphonon decay to the upper laser level, so the total energy required to excite a Nd ion to the upper laser level is reduced by ~4%. There is a corresponding decrease of 33% in the total heat generated from quantum defect. Pumping at 881 nm also increases the optical to optical efficiency of the Nd:YLF laser [15]. In addition, the relatively weak absorption at 881 nm is such that the absorption is distributed uniformly over the length of the crystal, so that the local temperature rise in the crystal is minimized. Regarding the relatively-low fracture limit for Nd:YLF, many works have now overcome this problem achieving high output power CW lasers using Nd:YLF [16, 17].

There have been two main reports to date of CW Raman lasers based on Nd:YLF. First, Savitski *et al.* [6] used a Nd:YLF laser module (side pumped with 153 W of diode power) operating at 1047 nm to intracavity pump a diamond crystal, obtaining 5.1 W of CW output at 1217 nm (M^2~1.1). In this same system, they also pumped a KGW crystal, obtaining 6.1 W at 1139 nm (M^2~5.5). This is the highest reported output power for a CW Raman laser reported to date, and the corresponding diode to Stokes conversion efficiency was a modest 4%. The second Nd:YLF-based laser was reported by Bu *et al.* [18]; it combined the 1047 nm Nd:YLF fundamental, the 921 cm^{-1} Raman shift in a 30 mm long $SrWO_4$ crystal and frequency doubled in LBO to create a CW yellow laser source at 579 nm for ophthalmology. 889 mW was generated at a diode to yellow conversion efficiency of 5.8%.

In this work, our emphasis is on investigating how the thermal and optical properties of Nd:YLF can enhance the operation of CW Raman lasers. We report a Nd:YLF/KGW CW intracavity Raman laser where the Nd:YLF operates at 1053 nm fundamental. We chose KGW as the Raman-active crystal because it has similar Raman gain to the vanadates, ~4.5 cm/GW [19], used in self-Raman lasers to deliver the best intracavity frequency-doubled CW Raman laser results to date. We find that thermal lensing in our Nd:YLF/KGW CW Raman lasers is weak (as expected), thereby permitting lasers to be designed with cavity lengths of 25 cm and potentially much longer, and resulting in relatively high beam quality parameters (compared to self Raman lasers) of between 1.2 and 2.5. An advantage of KGW is the fact that it has two strong Raman lines at 768 cm^{-1} and at 901 cm^{-1}, with similar Raman gain, that can be accessed separately, just by orientation of the KGW. Given that, and the capacity of Nd:YLF to emit in two different wavelengths, it is therefore possible to obtain four different Stokes wavelengths with this system, 1139 nm, 1147 nm, 1156 nm and 1163 nm. Consequently many visible lines from the green to the yellow-orange range of the visible may be achieved by second harmonic generation (SHG) or sum frequency generation (SFG) as shown in Fig. 1. Here we demonstrate two of those combinations by using the 1053 nm fundamental wavelength and then, shifting to 1147 nm (0.70 W-CW) and 1163 nm (0.95 W-CW). In addition, we have demonstrated the SHG and SFG of those new wavelengths, obtaining emission at 549 nm (0.65 W-CW), 552 nm (1.90 W-CW), 573 nm (0.60 W-CW)

#161668 - $15.00 USD Received 18 Jan 2012; revised 3 Apr 2012; accepted 4 Apr 2012; published 16 Apr 2012

and 581 nm (1.10 W-CW). As this is the first time a Raman laser has been investigated using the 1053 nm fundamental transition of Nd:YLF, we were able to demonstrate two wavelengths not reported before in crystalline Raman lasers, 549 nm and 552 nm.

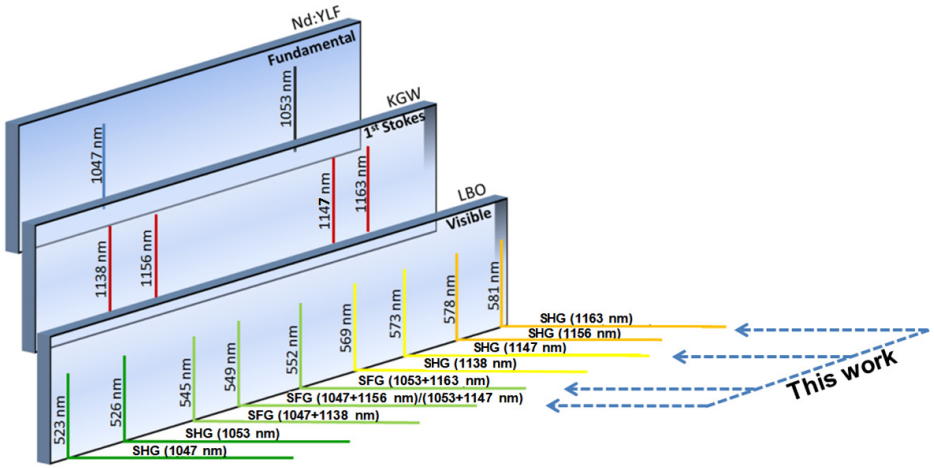

Fig. 1. Wavelengths that can be generate using the combination of Nd:YLF/KGW/LBO.

2. Lasers experimental setup

The lasers described in this section were all pumped with the same pump source, a 60 W fiber coupled diode laser (LIMO) emitting at 880 nm, with a fiber diameter of 100 μm and a numerical aperture (N.A.) of 0.22. A 25 mm focal length lens was used for collimation and a 125 mm lens was used for focusing, delivering a pump spot of 500 μm of diameter in the Nd:YLF laser crystal. The diode output wavelength was temperature-tuned to 881 nm, in order to match an absorption peak of the Nd:YLF crystal [15]. The fraction of pump power absorbed in the 15 mm crystal was 43%, and this is something that could be optimized in the future, for example by double-passing the pump. Direct pumping has two main benefits: first, a 33% reduction in heat by eliminating the multiphonon decay from the pump level to the upper laser level, and second, as the absorption coefficient at this wavelength is smaller than the ones at conventional pump wavelengths, distributing the absorption over the whole length of the crystal so that the local temperature rise in the crystal is minimized. A chopper was placed after the diode fiber in order to investigate quasi-CW operation; in this case, the chopper was operated with 50% duty cycle and frequency of 850 Hz, so the thermal lens was approximately 50% of the CW case. In this mode of operation we can predict the CW output power that could be achieved by pumping the crystal harder, without taking the risk of a thermal fracture.

We used a Nd:YLF plane-Brewster cut crystal with 1 at% Nd^{3+} doping concentration and dimensions of 4×4×15 mm^3. The 1 at% doping concentration was chosen in order to have a reasonable absorption at 881 nm and also to minimize energy transfer upconversion (ETU) [20]. The crystal's flat face was coated for high transmission (T>95%) at 881 nm, with low reflectivity for fundamental 1047/1053 nm (R<0.2%) and first Stokes wavelength range 1135-1170 nm (R<0.1%). The Brewster-cut on the other face introduced losses for 1047 nm, thereby enabling the 1053 nm fundamental wavelength to oscillate without competition. We chose 1053 nm as the fundamental wavelength because it generally has a weaker thermal lens than 1047 nm [14] and was therefore more likely to deliver good beam qualities and freedom to design long cavities. There are resonator designs that allow the laser to operate under strong thermal lensing, such as telescopic resonators [21], however, they typically operate only for a short range of pump powers, and generally introduce extra optics to the resonator, increasing the intracavity losses. Accordingly, we did not investigate their use here.

#161668 - $15.00 USD Received 18 Jan 2012; revised 3 Apr 2012; accepted 4 Apr 2012; published 16 Apr 2012

We used a 5×5×24 mm KGW crystal as the Raman-active medium. It was AR-coated at the fundamental and Stokes wavelengths (R<0.1% at 1053-1170 nm), and cut for propagation along the N_p axis. The Raman spectrum for KGW is complex [22] and Fig. 2 shows the Raman spectra measured (using a Renishaw InVia Reflex microRaman spectrometer with resolution 2 cm^{-1}) for the two orientations we used in this work. The KGW crystal was placed in a copper mount that could be rotated in order to access either the 901 cm^{-1} shift (fundamental and Stokes polarization parallel to the N_m refractive index axis) or the 768 cm^{-1} shift (fundamental and Stokes polarization parallel to the N_g refractive index axis). Table 1 shows the combinations of fundamental, Stokes, yellow and lime-green emission generated using the two Raman shifts.

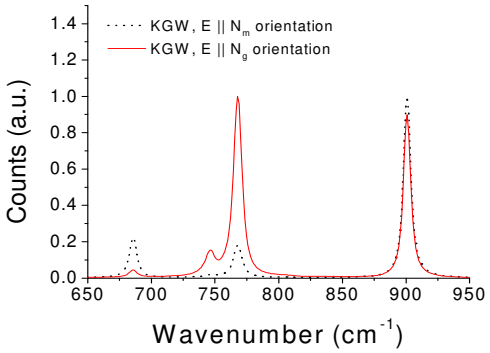

Fig. 2. Raman spectra at the two orientations used for the laser.

Table 1. 1st Stokes, SHG and SFG Wavelengths Generated by Nd:YLF/KGW System

Shift	Fundamental	1st Stokes	SHG	SFG
768 cm^{-1}	1053 nm	1147 nm	573 nm	549 nm
901 cm^{-1}		1163 nm	581 nm	552 nm

The cavity used to obtain 1st Stokes laser emission is shown in Fig. 3. The input mirror had high reflectivity (>99.99%) at 1053 nm, 1147 nm and 1163 nm, and high transmission (T>90%) at 880 nm, with 400 mm radius of curvature (ROC). The output coupler (O.C.) for the 1st Stokes had a R>99.99% at 1053 nm, 0.2% transmission at 1163 nm and 0.1% transmission at 1147 nm, with 250 mm of ROC. The distance from the last end face of the KGW to the O.C. was 115 mm and the overall cavity length was 160 mm. The TEM_{00} resonator mode had 420 μm diameter in the laser crystal and 400 μm diameter in the Raman crystal, calculated using an ABCD resonator model (LASCAD GmbH).

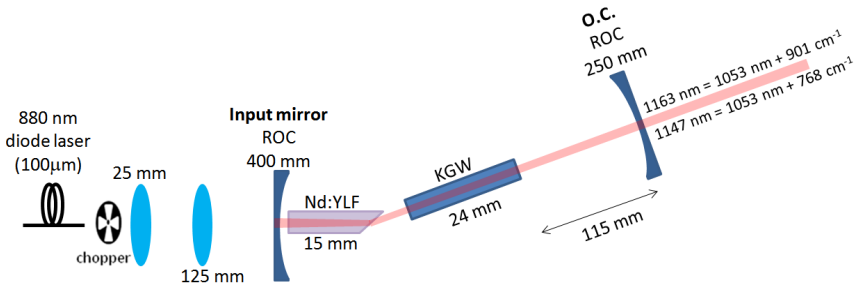

Fig. 3. Nd:YLF/KGW 1st Stokes laser setup.

#161668 - $15.00 USD Received 18 Jan 2012; revised 3 Apr 2012; accepted 4 Apr 2012; published 16 Apr 2012

A lithium triborate (LBO) crystal (4×4×10 mm^3) was used for intracavity SHG/SFG. It was cut for Type I non-critical phase-matching, and AR-coated at the fundamental, Stokes and SHG/SFG wavelengths (R<0.1% at 1053-1170 nm and T>95% at 570-590 nm). The LBO crystal was positioned next to the KGW, as shown in Fig. 4, and temperature tuned to 63°C for 573 nm or 50°C for 581 nm. The TEM_{00} resonator mode diameters were 380 μm, 366 μm and 368 μm respectively in the laser, Raman and doubling crystals. The curved (200 mm ROC) output coupler had high reflectivity, R>99.99% at the fundamental and Stokes wavelengths and high transmission, ranging from 80 to 95%, at the yellow and lime-green wavelengths. An intracavity mirror was also introduced between the KGW and LBO crystals in order to redirect the backwards propagating yellow beam toward the O.C. This intracavity mirror had an antireflective (AR) coating at 1053 nm (R<0.1%), 1147 nm and 1163 nm (R<0.1%), and a HR at 573 nm and 581 nm (R>98%).

For the SFG cases, 549 nm and 552 nm, the same configuration was used. The temperatures of the LBO crystal required for phase matching were 109°C for 549 nm and 101°C for 552 nm.

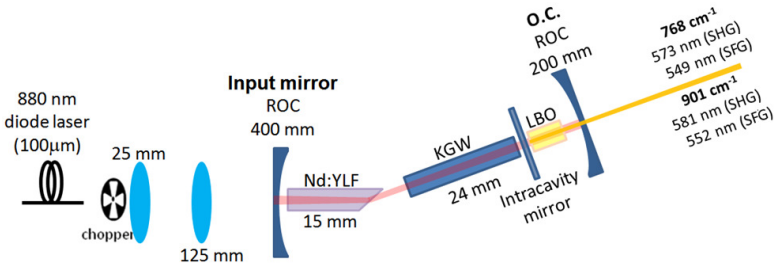

Fig. 4. Nd:YLF/KGW/LBO yellow and lime-green laser setup.

3. Results

The results are presented in three different sections, the first one concerns the thermal lens characterization, and the following two sections concern laser operation using the two different Stokes shifts for KGW (768 cm^{-1} and 901 cm^{-1}).

3.1. Estimating the thermal lens

In order to estimate the thermal lens of the Nd:YLF crystal, we built a high-Q, plane-parallel cavity (using a Nd:YLF crystal without Brewster cut) for the 1053 nm field with length 120 mm, and made observations about resonator stability. Strong laser emission from the flat-flat resonator indicated that the thermal lens was positive. Next, we focused the 881 nm beam to a 300 μm diameter spot into the crystal, and found that the laser operated stably for absorbed pump powers up to 14 W, above which the laser output decreased and could not be sustained. Accordingly, we concluded that the focal length of the thermal lens in the Nd:YLF was 120 mm under these conditions, in the plane which corresponds to the strongest thermal lensing.

From [23], the thermal lens focal length depends on the square of the pump radius, ω_p, and we can thereby infer that the focal length for the 500 μm diameter used in our Raman lasers is around 330 mm. This is consistent with our observations using a 500 μm pump diameter and the resonator shown in Fig. 3, in which stable output power at the fundamental was obtained for pump powers up to 17.5 W and for resonator lengths as long as 265 mm. Inserting the Raman crystal, we observed stable Stokes oscillation for cavity lengths from 45 mm to 250 mm. Accordingly, for the lasers described in the following sections, the resonators operated well away from the regions of resonator instability. Moreover there is clearly scope in the future for designing longer resonators to optimize laser performance.

#161668 - $15.00 USD Received 18 Jan 2012; revised 3 Apr 2012; accepted 4 Apr 2012; published 16 Apr 2012

3.2. Laser operating at the 901 cm^{-1} shift

When the KGW was oriented to access the 901 cm^{-1} shift, the 1st Stokes laser delivered a maximum CW power of 0.95 W at 1163 nm for an absorbed pump power of 12.3 W. The beam quality was measured to have M^2 of 1.49. For quasi-CW operation 1.56 W of peak power was obtained for 21 W absorbed pump power. Figure 5(a) shows the output power performance of this laser. The Stokes beam profile was elliptical, due to the Brewster angle in the cavity, and the M^2 and beam sizes mentioned are average values for the two planes. We did not measure the beam quality of the fundamental beam (1053 nm) because the mirrors have a very high reflectivity at this wavelength (>99.9%), thus, the residual power leaking from the cavity was not enough to make a good M^2 measurement.

When the 10 mm LBO crystal temperature was tuned to 50 °C for the SHG of 1163 nm, a CW output power of 1.10 W at 581 nm was obtained, with M^2 of 1.93. In quasi-CW mode, 1.65 W of peak power was obtained, Fig. 5(b). It is interesting to note that the powers in the visible are higher than in the infrared and this is attributed to the fact we were not using the optimum output coupling for the 1st Stokes.

When the LBO crystal was tuned to 101°C for SFG of 1053 nm and 1163 nm, we obtained 1.90 W CW at 552 nm for 13 W of absorbed pump power. The corresponding beam quality was M^2~2.01. In quasi-CW operation, 3.12 W of peak power was achieved for 20 W of pump. Figure 5(c) shows the output power performance for this laser.

The spectral linewidths (full width at half-maximum) of the fundamental, first Stokes and visible lines were measured to be 0.3 nm.

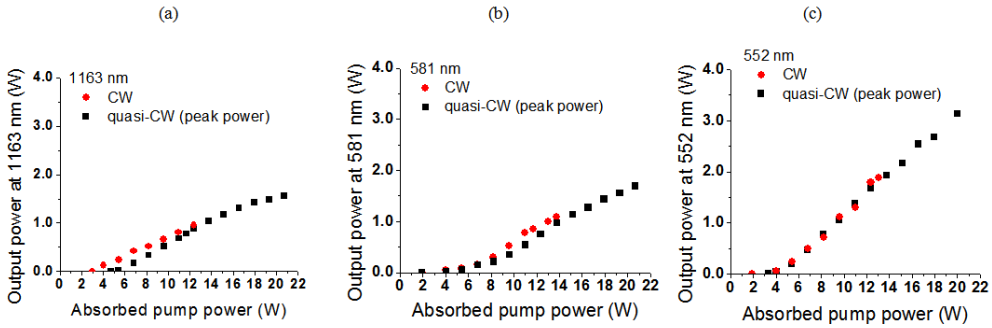

Fig. 5. Output power as a function of absorbed pump power for (a) 1163 nm, (b) 581 nm and (c) 552 nm.

3.3. Laser operating with the 768 cm^{-1} shift

When the KGW crystal was rotated to access the best gain for the 768 cm^{-1} shift, the first Stokes laser delivered 0.70 W CW power at 1147 nm for 13 W of absorbed pump power and for quasi-CW operation, 1.20 W of peak power for 20 W absorbed pump power, as shown in Fig. 6(a). The beam quality was measured to be M^2~1.44.

When optimized for frequency doubling the 1st Stokes, we obtained 0.60 W CW power at 573 nm for an absorbed pump power of 13 W (see Fig. 6(b)) and the corresponding beam quality was measured to be M^2~1.76. In quasi-CW operation the maximum peak yellow power was 1.25 W for 18 W of pump power. At higher (18-20 W) pump powers the 901 cm^{-1} Raman transition began to compete. Looking at the Raman spectra in Fig. 2, we can see that for this orientation the 901 cm^{-1} and 768 cm^{-1} lines have similar intensities, with the 768 cm^{-1} only slightly stronger. The competition arises because there are losses for the 768 cm^{-1} shift through the SHG process, but no such losses for the 901 cm^{-1} shift.

When optimized for sum frequency to generate 549 nm, a maximum power of 0.65 W was achieved in CW regime and 1.20 W peak power when chopped, as seen in Fig. 6(c).

#161668 - $15.00 USD Received 18 Jan 2012; revised 3 Apr 2012; accepted 4 Apr 2012; published 16 Apr 2012

Unfortunately coating damage occurred on the KGW crystal and the low thresholds obtained previously could not be realized. It is very likely that considerably higher output powers could be achieved at 549 nm using a KGW crystal with un-damaged coatings.

The spectral linewidths (full width at half-maximum) of the fundamental, first Stokes and visible lines were measured to be 0.3 nm.

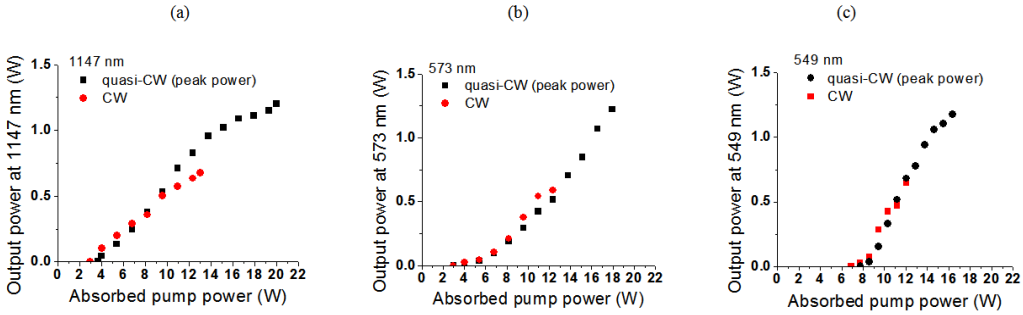

Fig. 6. Output power as a function of absorbed pump power for (a) 1147 nm, (b) 573 nm and (c) 549 nm.

4. Discussion

The laser performance shown in Fig. 5 and 6 is very good in terms of output power and efficiency, particularly when we consider that the coatings on the crystals and mirrors were specifically designed for a system having a 1064 nm fundamental wavelength (ie. not 1053 nm). The lasers reported here operate over a useful range of wavelengths and output powers, with good efficiencies. The highest conversion efficiency (with respect to absorbed pump power) reported here is 14% in the case of SFG to 552 nm, and this can be compared against 20% obtained in a self-Raman Nd:$GdVO_4$ laser with SFG to 559 nm [4], which is the highest efficiency reported in the literature. The higher efficiency in [4] can be attributed to lower resonator losses, enabled by very low loss AR-coatings on the crystals. For the yellow, we achieved a conversion efficiency of 7.8% for generation of 581 nm, somewhat lower than the highest-reported conversion efficiency (17%) for a self-Raman [8] operating at 586 nm, but again the difference is due to extremely low resonator losses in [8]. In the case of the 1st Stokes, our conversion efficiency of 7.3% when generating first Stokes output at 1163 nm can be compared against 13.8% for the best CW self-Raman performance, from a composite Nd:KGW/KGW laser operating at 1181 nm [10]. Furthermore, the Nd:YLF Raman lasers we have demonstrated had good beam quality, with M^2~1.49 for the 1st Stokes laser at 1163 nm, and with $M^2 \leq 2$ for CW operation at 1147 nm and in the visible at 581 nm and at 552 nm. This beam quality is considerably better than for the Nd:$GdVO_4$ self-Raman lasers in which the beam quality for the sum frequency was M^2~10 [4], and for the second harmonic was M^2~6 [12], both at maximum pump power. The good beam quality reported here for Nd:YLF Raman lasers is a consequence of the much weaker thermal lensing, since the beam quality is strongly linked to thermal lensing, which in the case of self-Raman laser is typically very strong and abberated.

We can also compare our results to other Raman lasers reported using Nd:YLF. Savitski *et al*. reported the highest output power of 6.1 W [6] for any CW Raman laser, by combining the 1047 nm fundamental from Nd:YLF and the 768 cm^{-1} shift in KGW. However, the overall diode to first Stokes efficiency of ~4% was substantially lower than the 7.3% reported here, and also the beam quality, M_x^2 ~5 and M_y^2 ~6, is not so good as the M^2 ~1.5 reported here. Interestingly, the beam quality they found using diamond (instead of KGW) was an excellent M_x^2~1.1 and M_y^2 ~1.2, which given the very high thermal conductivity of diamond, suggests that some of the beam degradation occurs in the Raman crystal. In the work of Bu. *et al*. [18], the (absorbed) diode to yellow conversion efficiency is estimated to be 7.4%, quite similar to

#161668 - $15.00 USD Received 18 Jan 2012; revised 3 Apr 2012; accepted 4 Apr 2012; published 16 Apr 2012

the conversion efficiency we have obtained (7.8%). An attractive feature used in [18] is the coupled cavity setup. This reduces considerably the intracavity losses for the Stokes field, yielding lower thresholds for SRS: 1.35 W compared to our lowest threshold of 2 W for yellow (581 nm).

We anticipate substantial improvements in efficiency will be possible in the future by improving the characteristics of the mirror and crystal coatings, particularly the AR-coatings on the Raman crystals and the visible transmission of the output coupler. For all the cases investigated here, the laser performance was superior when using the 901 cm^{-1} shift, compared to the 768 cm^{-1} shift. While the 1163 nm laser provided a maximum CW power near 1 W, the 1147 nm only achieved about 700 mW. For the visible, the 581 nm laser delivered more than 1 W with a threshold of 2 W of absorbed power, while the 573 nm laser provided a maximum of 600 mW with a threshold of 3 W of absorbed power. These differing performances could be due to differences, either in Raman gain or resonator losses, for the various wavelengths. According to the literature [24] as well as our measured spectrum in Fig. 2, the 768cm^{-1} shift has higher Raman gain than 901 cm^{-1}, but we believe such a difference is not enough to explain the different performances we have observed. Considering all the mirror and crystal coatings, we found the round trip losses for both Stokes wavelengths to be similar, with the 1147 nm losing 0.1% more power per round trip than the 1163 nm, which may contribute to the small difference between their thresholds. Moreover the output coupler has a transmission of about 0.1% at 1147 nm and 0.2% at 1163 nm, this higher output coupling contributes to the higher power at 1163 nm. The maximum powers at 1147 nm were slightly limited by the onset of competition between the 901 cm^{-1} and 768 cm^{-1} shifts for absorbed pump powers above 18 W. With regard to the different output powers that were obtained in the yellow, we note that the O.C. mirror has about 20% of reflectivity at 573 nm and <5% at 581 nm, and this is likely to be the main cause for the reduced performance of 573 nm when compared to 581 nm. The powers at the two sum frequency wavelengths cannot be compared due to the crystal damage that occurred when optimising performance at 549 nm.

Our observations of resonator stability, for fundamental oscillation only, in resonators up to 265 mm long (17.5 W of absorbed power/500 μm pump diameter) show that thermal lensing is quite weak in our Nd:YLF crystal, with a focal length of ~330 mm at maximum pump power. This is much weaker than what is typically found in CW Nd:$GdVO_4$ self Raman lasers, such as in [11] where it is 60 mm long (18 W of absorbed power, 808 nm/400 μm pump diameter) and in [12] where it is 70 mm long (20 W of absorbed power, 880 nm/400 μm pump diameter). The relative-weakness of the thermal lens in Nd:YLF is also apparent in the laser performance under CW and quasi-CW (50% duty cycle) operation of our Nd:YLF Raman lasers. The performances were very similar for up to ~14 W pump power, the maximum CW pump power that was used, indicating that an approximately 50% decrease in thermal lens, made little difference to the mode sizes in the laser and Raman crystals, and ultimately the output power. This is quite different to the scenario of self Raman lasers such as in Nd:$GdVO_4$ [11] where strong thermal lensing, even in very short (few cm) resonators made the resonator become unstable (and the output power declines steeply) under CW pumping, while for quasi-CW (50% duty cycle) pumping, the output power continued to increase over the power range tested. In the future, the relatively long thermal lens in Nd:YLF will enable us to explore folded cavity designs that enable the mode sizes in the laser, Raman and doubling crystals to be optimized for higher conversion efficiencies and multi-Watt CW output powers across the range of wavelengths demonstrated here, as well as the set of wavelengths that can be accessed using the 1047 nm fundamental transition in Nd:YLF.

The output powers we have reported here for Nd:YLF Raman lasers are substantial, particularly in the visible: CW operation yielded up to 0.95 W in the near-ir (1163 nm) and 1.9 W in the visible (552 nm) quasi-CW operation at 50% duty cycle resulted in peak output powers up to 1.65 W in the near-ir (1163 nm) and over 3 W in the visible (552 nm). Higher peak powers would be achieved at lower duty cycles, and there are many applications for which modulated laser output is suitable. Our capacity to scale to higher powers has been constrained by the need to avoid fracture of the Nd:YLF. Here we note recent developments

#161668 - $15.00 USD Received 18 Jan 2012; revised 3 Apr 2012; accepted 4 Apr 2012; published 16 Apr 2012

in power-scaling CW Nd:YLF in which up to 60 W of output power at 1053 nm was demonstrated [17] by using large mode sizes in the Nd:YLF, and accordingly, we believe there is considerable potential for efficiently scaling Nd:YLF-based Raman lasers to much higher powers.

Yet another exciting possibility exists to build a low-noise, multi-Watt yellow laser, this possibility stemming from the broad (~360 GHz) emission band of Nd:YLF. Here the concept is to build a sufficiently-long Raman resonator that operates simultaneously on a large number (100s) of longitudinal modes, an approach previously used to solve the "green problem" [25, 26].

5. Conclusions

Nd:YLF is a suitable laser crystal for Raman lasers and CW output powers of 0.6 W to 1.9 W have been achieved in the near-infrared at 1147 nm and 1163 nm and visible at 549 nm, 552 nm, 573 nm and 581 nm. To the best of our knowledge, this is the first time a Raman laser has been investigated using the 1053 nm fundamental of Nd:YLF and as a consequence, it is the first time a crystalline Raman laser has been operated at this sequence of visible wavelengths. We have demonstrated that thermal lensing is quite weak, much less than for the self-Raman lasers, and this provides a strong platform for constructing efficient, multi-Watt Raman lasers with high beam quality.

Acknowledgements

Jonas is a CAPES scholar: Proc nº 5381/09-6.

#161668 - $15.00 USD Received 18 Jan 2012; revised 3 Apr 2012; accepted 4 Apr 2012; published 16 Apr 2012